

## Ultraviolet Absorption Spectra of $\text{Pr}^{3+}$ Ion in Alkaline-Earth Fluorides

EUGENE LOH

*Physical Sciences Department, Douglas Aircraft Company, Santa Monica, California*

(Received 11 January 1967)

The ultraviolet absorption spectra of  $\text{Pr}^{3+}$  in  $\text{CaF}_2$ ,  $\text{SrF}_2$ , and  $\text{BaF}_2$  have been measured at room and liquid-nitrogen temperatures. These spectra are similar to those of  $\text{Ce}^{3+}$  reported previously except that  $\text{Pr}^{3+}$  absorptions generally occur at higher photon energies. This general similarity between the uv absorption spectra of  $\text{Ce}^{3+}$  and  $\text{Pr}^{3+}$  in solids indicates that the crystal field is dominant in the higher configurations,  $5d$  and  $6s$ , of rare-earth ions in solids. For  $\text{Pr}^{3+}$  in  $\text{CaF}_2$  the three interconfigurational transitions are: (1)  $4f \rightarrow 5d$  between 44 000 and 69 000  $\text{cm}^{-1}$ ; (2) a possible  $4f \rightarrow 6s$  at  $\sim 76\,000$   $\text{cm}^{-1}$ ; (3) a charge transfer  $\text{F}^-(2p^6) \rightarrow \text{Pr}^{3+}(6s)$  near  $\sim 80\,000$   $\text{cm}^{-1}$ . Other effects, such as vibronics in the lowest  $4f \rightarrow 5d$  band and their concentration dependence, the effect of cluster formation on  $4f \rightarrow 5d$  bands, and the crystal effect on the free-ion data, are all similar to the previously reported data on  $\text{Ce}^{3+}$  in alkaline-earth fluorides. The cross section of  ${}^1S_0$  absorption of  $\text{Pr}^{3+}$  in  $\text{CaF}_2$  is estimated to be concentration-independent, which is consistent with the shielded character of  $4f \rightarrow 4f$  transitions. Absorption to the  ${}^1S_0$  state and the vibronics are also observed in  $\text{BaF}_2:\text{Pr}^{3+}$ .

### I. INTRODUCTION

AS a direct approach to the study of interconfigurational transitions of trivalent rare-earth ions in solids, we have previously presented the ultraviolet-absorption spectra of the simplest rare-earth ion  $\text{Ce}^{3+}(4f^1)$  in alkaline-earth fluorides.<sup>1</sup> The spectra<sup>1</sup> of  $\text{Ce}^{3+}$  show three types of transitions:  $4f \rightarrow 5d$  narrow bands, a broad and weak  $4f \rightarrow 6s$  band, and the charge transfer of  $\text{F}^-(2p^6) \rightarrow \text{Ce}^{3+}(6s)$  appearing as the apparent red shift of the absorption edge of the host crystal.

For comparison with the work on  $\text{Ce}^{3+}$ , we present here the uv absorption data of  $\text{Pr}^{3+}$  in alkaline-earth fluorides.  $\text{Pr}^{3+}(4f^2)$  follows  $\text{Ce}^{3+}(4f^1)$  in the rare-earth series. Except for the latter, it has the lowest  $4f \rightarrow 5d$  transition energy<sup>2</sup> among trivalent rare-earth ions. Therefore  $\text{Pr}^{3+}$  may show as many interconfigurational transitions as  $\text{Ce}^{3+}$  within the transparent region of the host crystal.  $\text{Pr}^{3+}$  is also one of the few trivalent rare-earth ions whose free-ion<sup>3</sup> data became available recently. The free-ion data are useful<sup>1</sup> in comparing the corresponding data of interconfigurational transitions in solids.

The uv absorption spectra of  $\text{Pr}^{3+}$  are similar to those of  $\text{Ce}^{3+}$ : (1) The  $4f \rightarrow 5d$  bands of  $\text{Pr}^{3+}$  are shifted  $\sim 13\,000$   $\text{cm}^{-1}$  upward in energy from the corresponding bands of  $\text{Ce}^{3+}$ . The relative oscillator strengths of these bands of  $\text{Pr}^{3+}$  in  $\text{CaF}_2$  are concentration-dependent because of cluster<sup>1</sup> formation as in the case of  $\text{Ce}^{3+}$  in  $\text{CaF}_2$  or  $\text{SrF}_2$ . The lowest  $4f \rightarrow 5d$  band of  $\text{Pr}^{3+}$  in  $\text{CaF}_2$  and  $\text{BaF}_2$  also develops vibronic structures at low temperature. (2) A possible hump at  $\sim 76\,000$   $\text{cm}^{-1}$  in the absorption spectra of  $\text{Pr}^{3+}$  in  $\text{CaF}_2$  suggests the presence of  $4f \rightarrow 6s$  absorption of  $\text{Pr}^{3+}$ . In  $\text{CaF}_2:\text{Ce}^{3+}$  the  $4f \rightarrow 6s$  absorption<sup>1</sup> of  $\text{Ce}^{3+}$  is indicated by a weak and broad band with maximum at  $\sim 70\,000$   $\text{cm}^{-1}$ . (3) The apparent red shift of the absorption edge of the host

crystal with increasing  $\text{Pr}^{3+}$  concentration suggests also the charge transfer<sup>1</sup> of  $\text{F}^-(2p^6) \rightarrow \text{Pr}^{3+}(6s)$ . These general similarities between the uv absorption spectra of  $\text{Ce}^{3+}$  and  $\text{Pr}^{3+}$  in solids indicate that the crystal field is dominant in the higher configurations  $5d$  and  $6s$  of rare-earth ions in solids.

There are, however, two complications occurring in the uv absorption spectra of  $\text{Pr}^{3+}$ . First is the coincidental appearance of the  ${}^1S_0$  level,<sup>4</sup> the highest  $4f \rightarrow 4f$  transition of  $\text{Pr}^{3+}$ , in the lowest  $4f \rightarrow 5d$  band of  $\text{Pr}^{3+}$  in  $\text{CaF}_2$ , and  $\text{BaF}_2$ . This may complicate the interpretation of the vibronic structure in this band at low temperature. Second is the lack of structure in the lowest  $4f \rightarrow 5d$  of  $\text{Pr}^{3+}$  in  $\text{SrF}_2$ . Neither vibronic structure nor  ${}^1S_0$  absorption is noticeable in  $\text{Pr}^{3+}$  doped  $\text{SrF}_2$ . The structure may be smeared out by some strain of unknown origin in  $\text{SrF}_2$  crystals.

We shall discuss the uv absorption spectra of  $\text{Pr}^{3+}$  in the order of increasing energy:  $4f \rightarrow 5d$ ,  $4f \rightarrow 6s$ , and charge transfer  $\text{F}^-(2p^6) \rightarrow \text{Pr}^{3+}(6s)$ .

### II. $4f \rightarrow 5d$ ABSORPTION OF SINGLE-ION $\text{Pr}^{3+}$ IN ALKALINE-EARTH FLUORIDES

The uv absorption spectra of  $\text{Pr}^{3+}$  in  $\text{CaF}_2$ ,  $\text{SrF}_2$ , and  $\text{BaF}_2$  crystals are shown in Figs. 1, 2, and 3, respectively. The spectra cover various concentrations of  $\text{Pr}^{3+}$  and were taken at both room and liquid-nitrogen temperatures. The spectra of  $\text{Pr}^{3+}$  in these three host crystals are similar in general. As in the case<sup>1</sup> of  $\text{BaF}_2:\text{Ce}^{3+}$ ,  $\text{BaF}_2:\text{Pr}^{3+}$  appears to be the simplest. Its spectra consist of two regions of absorption, a lowest band *A* below 50 000  $\text{cm}^{-1}$  and a high-energy band between 61 000 and 67 000  $\text{cm}^{-1}$ , called region *B*, as shown by curve 3 for  $\text{BaF}_2:0.005\%$   $\text{Pr}^{3+}$  in Fig. 3. The spectra of  $\text{SrF}_2:\text{Pr}^{3+}$  and  $\text{CaF}_2:\text{Pr}^{3+}$  are very similar to each other. They have additional absorption bands in the intermediate spectral region called *C*, between 50 000 and 61 000  $\text{cm}^{-1}$ . It will be shown later that as the concentration of  $\text{Pr}^{3+}$  in  $\text{CaF}_2$  increases, the absorption in the intermediate region *C* increases while

<sup>1</sup> E. Loh, Phys. Rev. **154**, 270 (1967).

<sup>2</sup> E. Loh, Phys. Rev. **147**, 332 (1966).

<sup>3</sup> J. Sugar, J. Opt. Soc. Am. **55**, 1058 (1965). H. M. Crosswhite, G. H. Dicke, and Wm. J. Carter, J. Chem. Phys. **43**, 2047 (1965).

<sup>4</sup> E. Loh, Phys. Rev. **140**, A1463 (1965).

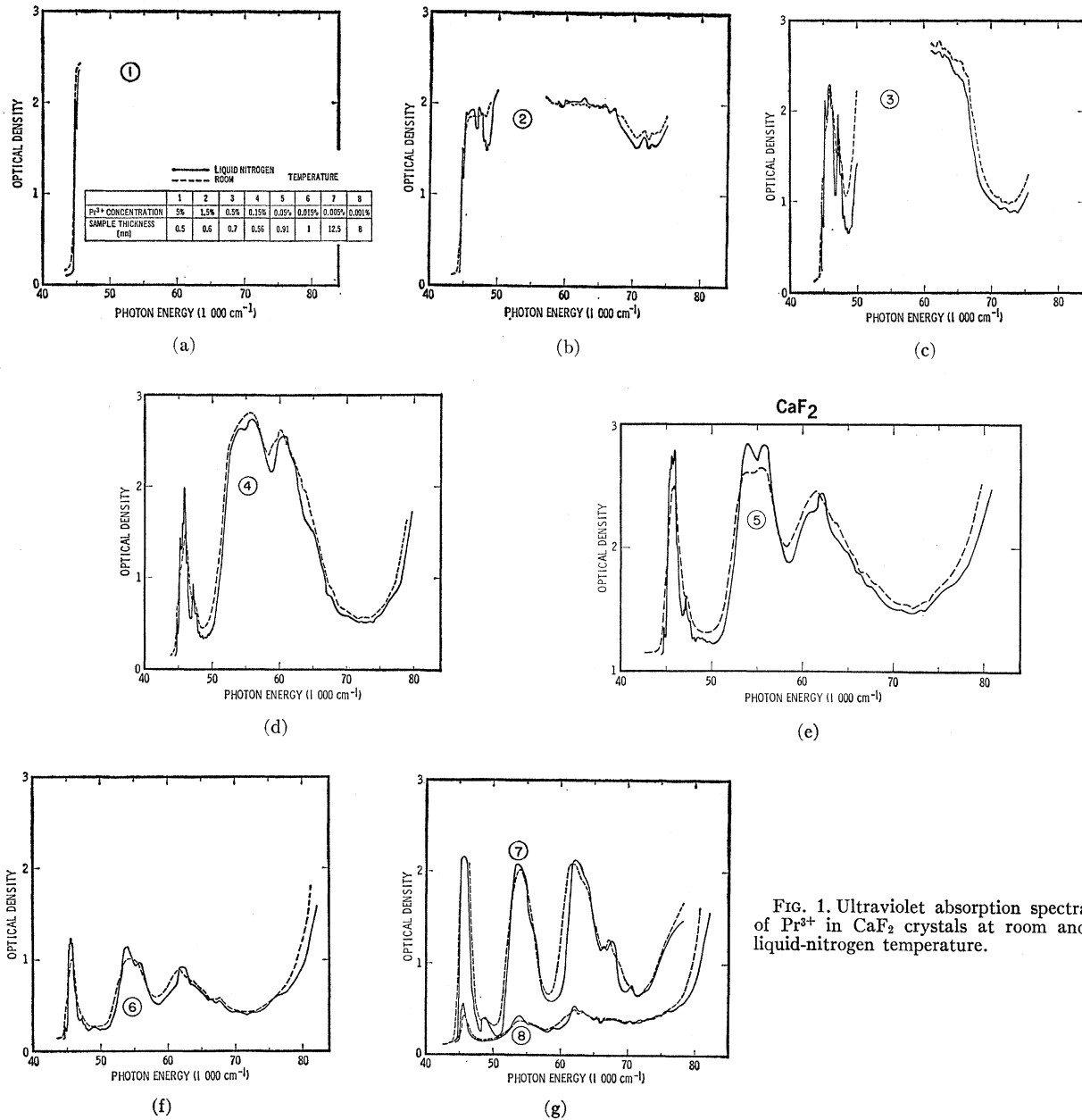


FIG. 1. Ultraviolet absorption spectra of  $\text{Pr}^{3+}$  in  $\text{CaF}_2$  crystals at room and liquid-nitrogen temperature.

that in the lowest-band *A* and high-energy bands *B* decreases. Following the example<sup>1</sup> of  $\text{Ce}^{3+}$ , we propose that bands *A* and *B* characterize the  $4f \rightarrow 5d$  absorption of single-ion  $\text{Pr}^{3+}$  while bands in region *C* are attributed to  $4f \rightarrow 5d$  absorption of cluster-ion  $\text{Pr}^{3+}$  in these crystals.

We first discuss the single-ion absorption. The absorption of cluster-ion  $\text{Pr}^{3+}$  will be discussed later in connection with the concentration dependence of  $\text{Pr}^{3+}$  absorption in  $\text{CaF}_2$ . From the interpretation<sup>1</sup> of the  $4f \rightarrow 5d$  absorption of single-ion  $\text{Ce}^{3+}$  in alkaline-earth fluorides, we assume also a tetragonal environment around  $\text{Pr}^{3+}$  due to the nearest-neighbor interstitial  $\text{F}^-$  as charge compensator. We assign the lowest band

as transitions from  $4f$  to  $|x^2 - y^2\rangle$  and three humps<sup>5</sup> in *B* as transitions from  $4f$  to  $|2z^2 - x^2 - y^2\rangle$ ,  $|xy\rangle$  and  $|yz\rangle$ , and  $|zx\rangle$  in the order of increasing energy.

Table I summarizes the experimental data<sup>5</sup> for the  $4f \rightarrow 5d$  transitions at liquid-nitrogen temperature. The

<sup>5</sup> The humps in the band *B* between 61 000 and 67 000  $\text{cm}^{-1}$  in  $\text{Pr}^{3+}$  spectra are not as prominent, and therefore their spectral locations are not as accurate, as the corresponding peaks (Ref. 1) of  $\text{Ce}^{3+}$  in the bands between 47 000 and 56 000  $\text{cm}^{-1}$ . In the high-energy region uv spectra are frequently of marginal quality because the quality of the crystal, the constancy of detecting phosphors, and the cleanness of the experiment are critical in the vacuum uv region. The stability of uv sources becomes more important at energies above 60 000  $\text{cm}^{-1}$ , where the hydrogen source emits line, instead of continuous, spectra.

data are assigned as components of  $5d$  orbitals in a tetragonal environment. The right portion of the table lists the centroids of  $e_g$ ,  $t_{2g}$ , and  $5d$  of  $\text{Pr}^{3+}$  as deduced from the experimental data. Values of crystal-field strength  $10 Dq$  are listed in the last column of the table as the energy difference between  $e_g$  and  $t_{2g}$ .

The effects of low temperature on the  $4f \rightarrow 5d$  absorption spectra are the sharpening of absorption bands, the increase in separation between the two  $e_g$  bands,  $|x^2-y^2\rangle$  and  $|2z^2-x^2-y^2\rangle$ , and the appearance of vibronic structure in the lowest band  $|x^2-y^2\rangle$ . Figure 4, with an enlarged energy scale for clarity, shows the vibronic structure in the  $|x^2-y^2\rangle$  band of  $\text{Pr}^{3+}$  in  $\text{CaF}_2$  for the concentration range from 0.001% to 5% at liquid-nitrogen temperature. The locations of humps in the spectra are tabulated in the first part of Table II for the low-concentration region from  $\sim 0.015\%$  to  $\sim 0.05\%$  and in the second part of Table II for the medium-concentration range from  $\sim 0.15\%$  to  $\sim 0.5\%$ . The data in this table shows that the vibronics consist of two frequency intervals. A larger interval  $\omega_1$  appears between "major humps" at  $\nu_j$ , marked by long lines in Fig. 4, and a smaller interval  $\omega_2$  separates "minor humps" at  $\nu_i$ , marked by short lines in Fig. 4, within the interval  $\omega_1$ . Wagner and Bron<sup>6</sup> in analyzing their vibronic data of divalent rare-earth ions in alkali halides have interpreted  $\omega_1$  and  $\omega_2$  as the out-of-phase and in-phase, respectively, resonance frequencies of pseudolocalized vibrations occurring at the divalent rare-earth defect in the monovalent host crystal. They also related  $\omega_1$  as being slightly larger than the longitudinal optical branch  $\nu_{LO}$  of the host lattice and  $\omega_2$  as being slightly lower than the transverse acoustical

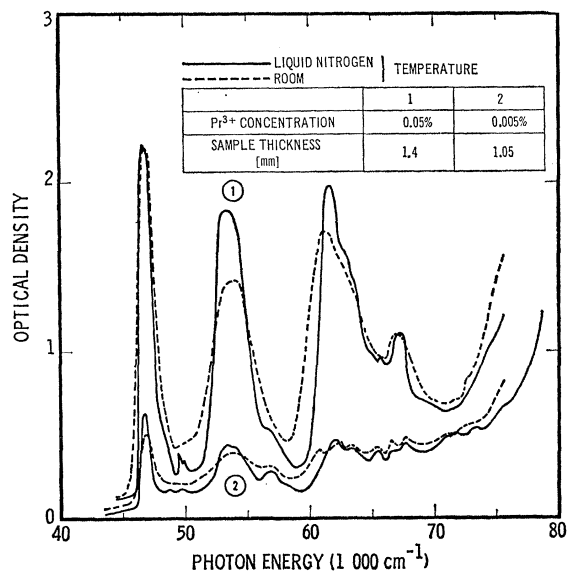


FIG. 2. Ultraviolet-absorption spectra of  $\text{Pr}^{3+}$  in  $\text{SrF}_2$  crystals at room and liquid-nitrogen temperature.

<sup>6</sup> M. Wagner and W. E. Bron, Phys. Rev. **139**, A223 (1965).

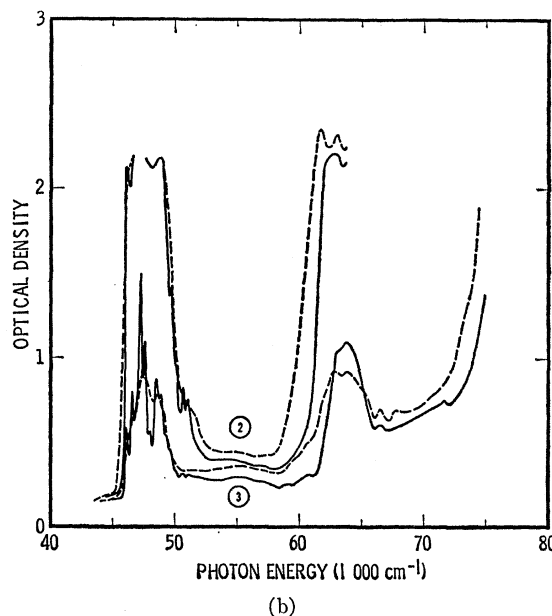
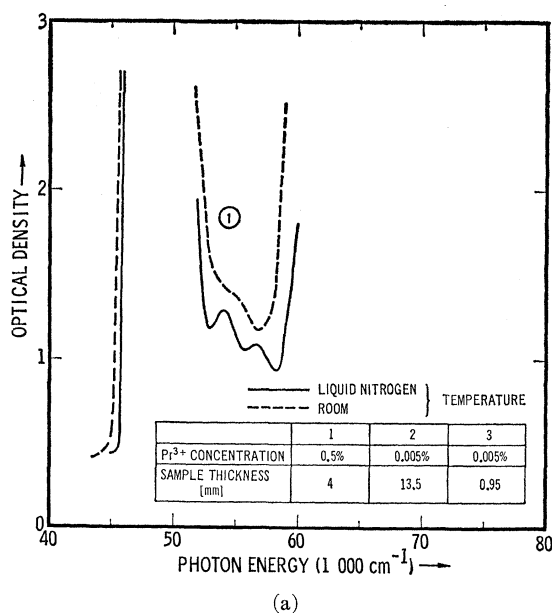


FIG. 3. Ultraviolet-absorption spectra of  $\text{Pr}^{3+}$  in  $\text{BaF}_2$  crystals at room and liquid-nitrogen temperature.

branch<sup>7</sup>  $\nu_{TA}$  of the host crystal. Values of  $\omega_1$ ,  $\sim 460 \text{ cm}^{-1} = \nu_{LO}$ , and  $\omega_2$ ,  $\sim 150 \text{ cm}^{-1}$ , for samples in the low  $\text{Pr}^{3+}$  concentration region, (see the first part of Table II or curve 8 to 5 in Fig. 4) are about the same as the corresponding values<sup>1</sup> of 0.005%  $\text{Ce}^{3+}$  in  $\text{CaF}_2$  which have been interpreted<sup>1</sup> by the vibronic model<sup>6</sup> of Bron and Wagner. As concentration of  $\text{Pr}^{3+}$  in  $\text{CaF}_2$  is raised to the medium-concentration region, 0.15% to 0.5%, the "major humps" remain at  $\nu_j$  (as shown by curves 3 and 4 in Fig. 4 or the second part of Table II) and the value of  $\omega_1 \approx 450 \text{ cm}^{-1}$  persists. The interval  $\omega_2$ ,

<sup>7</sup> This quantity was called  $\nu_{ao}$  in Refs. 1 and 7.

TABLE I.  $5d$  Levels and crystal-field strength  $10Dq$  for single-ion  $\text{Pr}^{3+}$  in alkaline-earth fluorides.

Host crystal	Experimental data ( $10^3 \text{ cm}^{-1}$ ) assigned as tetragonal components of $5d$ orbital				Deduced values ( $10^3 \text{ cm}^{-1}$ )			Crystal-field strength $10Dq$
	$x^2-y^2$	$2z^2-x^2-y^2$	$xy$	$yz$ and $zx$	Cubic $e_g$	Spherical $t_{2g}$	Spherical $5d$	
$\text{CaF}_2$	45.6	62	65	67.6	53.8	66.7	61.6	12.9
$\text{SrF}_2$	46.8	61.8	63.5	67.2	54.3	66	61.3	11.7
$\text{BaF}_2$	47.3	63	63.8	66.5	55.2	65.6	61.4	10.4

TABLE II. Vibronic structure of  $\text{Pr}^{3+}$  in alkaline-earth fluorides at liquid-nitrogen temperature (frequency in  $10^3 \text{ cm}^{-1}$ ).

	$\nu_j$	$\omega_1$ ( $=\Delta\nu_j$ )	$\nu_{\text{LO}}$	$\nu_i$	$\omega_2$ ( $=\nu_i-\nu_j$ OR $\Delta\nu_i$ )	$\nu_{\text{TA}}$	$\nu_{\text{TO}}$
0.015% to 0.05% $\text{Pr}^{3+}$ in $\text{CaF}_2$							
44.76 <sup>a</sup>	45 <sup>b</sup>			45.17	0.17	0.07 <sup>c</sup>	
	45.46	0.46	0.46 <sup>e</sup>	45.32	0.15		
	45.89	0.43		45.62	0.16		
	46.34	0.45		45.75	0.13		
	46.78 <sup>b</sup>	0.44		46.05	0.16		
	47.19 <sup>e</sup>	0.41		...			
	47.64	0.45		47.02	0.24 <sup>d</sup>		
	48.03	0.39		47.44	0.25 <sup>d</sup>		
	48.47	0.44					
	48.92	0.45					
0.15% to 0.5% $\text{Pr}^{3+}$ in $\text{CaF}_2$							
44.78 <sup>a</sup>	45 <sup>b</sup>			45.27	0.27		0.26 <sup>e</sup>
	45.45	0.45	0.46 <sup>e</sup>	45.68	0.23		
	45.90	0.45		46.12	0.22		
	46.33	0.43		46.59	0.26		
	46.78	0.45		47.02	0.24		
	47.19 <sup>e</sup>	0.41		47.44	0.25		
	47.64	0.45					
	48.03	0.39					
	48.44	0.41					
	48.9	0.46					
	49.35	0.45					
0.005% <sup>f</sup> $\text{Pr}^{3+}$ in $\text{BaF}_2$							
46.11 <sup>a</sup>	46.56						
	46.92	0.36	0.33				
	47.24 <sup>e</sup>	0.32					
	47.6	0.36					
	48	0.4					
	48.52	0.52					
	48.88	0.36					
	49.33	0.45					
	49.67	0.34					
	50.17	0.5					
	50.68	0.51					
	51.06	0.38					

<sup>a</sup> This low-energy peak is strong. It is, however, not separated by  $\omega_1$  from other major humps. In  $\text{CaF}_2$  it is only  $\sim 200 \text{ cm}^{-1}$  lower in energy from the next major hump. This peak shifts upward in energy with increasing  $\text{Pr}^{3+}$  concentration. It is also observed in  $\text{CaF}_2$  by M. H. Crozier [Bull. Am. Phys. Soc. **9**, 631 (1964)].

<sup>b</sup> It becomes obvious at 0.5%  $\text{Pr}^{3+}$  concentration, curve 3 in Fig. 4.

<sup>c</sup> The lattice data are taken from W. Kaiser, W. G. Spitzer, R. H. Kaiser,

and L. E. Howarth, Phys. Rev. **127**, 1950 (1962). From their infrared data, the deduced value of  $\nu_{\text{TA}}=71 \text{ cm}^{-1}$  for  $\text{CaF}_2$  seems to be anomalously lower than that of  $\text{SrF}_2$  and  $\text{BaF}_2$  with  $\nu_{\text{TA}}=99$  and  $94 \text{ cm}^{-1}$ , respectively.

<sup>d</sup> Here the value of  $\omega_2$  is close to  $\nu_{\text{TO}}$  as in the region of medium concentration of  $\text{Pr}^{3+}$ .

<sup>e</sup>  $^1S_0$  absorption.

<sup>f</sup> The absorption spectrum of 0.01%  $\text{Pr}^{3+}$  in  $\text{BaF}_2$  is similar.

however, expands to  $\sim 250 \text{ cm}^{-1}$  and consequently only one "minor hump" can be contained in each major interval  $\omega_1$ . It is interesting to note that  $\omega_2 \approx 250 \text{ cm}^{-1}$  in the medium-concentration region is close to the transverse optical-branch frequency  $\nu_{\text{TO}} = 260 \text{ cm}^{-1}$  of  $\text{CaF}_2$ .

We speculate on the origin of the increase of  $\omega_2$  from its value near  $\nu_{\text{TA}}$  at low  $\text{Pr}^{3+}$  concentration to that near  $\nu_{\text{TO}}$  at medium  $\text{Pr}^{3+}$  concentration as follows. At low concentrations of  $\text{Pr}^{3+}$  in  $\text{CaF}_2$ , the frequency  $\omega_2$  corresponds to the in-phase resonance of  $\text{Pr}^{3+}$  with respect to four substitutional  $\text{F}^-$  ions which are in the same general direction from  $\text{Pr}^{3+}$  as its charge compensator—interstitial  $\text{F}^-$ . This is similar to the situation of divalent rare-earth ions in the charge-compensated monovalent alkali halides as proposed by Bron and Wagner.<sup>6</sup> As  $\text{Pr}^{3+}$  concentration in  $\text{CaF}_2$  increases, the direct effect on  $\text{Pr}^{3+}$  from its charge compensator is gradually diminished because of the proximity of other interstitial  $\text{F}^-$  from the neighboring  $\text{Pr}^{3+}$  ions such as those in the cluster.<sup>1</sup> The presence of two or more charge compensators around  $\text{Pr}^{3+}$  will suppress the in-phase resonance, with frequency  $\omega_2 \approx \nu_{\text{TA}}$ , at rare-earth defects because of the disappearance of a preferential direction. In this stiffened environment of  $\text{Pr}^{3+}$  due to the presence of several neighboring interstitial  $\text{F}^-$  ions in the region of medium  $\text{Pr}^{3+}$  concentration,  $\omega_2$  tends to associate with a higher resonance frequency such as the transverse optical branch  $\nu_{\text{TO}}$ . By the same reasoning, we may expect that  $\omega_2$  of divalent rare-earth ions ( $\text{RE}^{2+}$ ) in alkali halides will also increase from the value near  $\nu_{\text{TA}}$  to that near  $\nu_{\text{TO}}$  as  $\text{RE}^{2+}$  concentration in a monovalent host increases. Some variations of  $\omega_2$  for  $\text{RE}^{2+}$  in alkali halides as listed in Table III of Ref. 6 may be attributed to such changes in local environment around the  $\text{RE}^{2+}$ . In  $\text{Sm}^{2+}$ -doped  $\text{CaF}_2$ , where there is no preferential direction around  $\text{RE}^{2+}$  because of the absence of the charge compensator,  $\nu_{\text{TO}}$  instead of  $\nu_{\text{TA}}$  is known<sup>8</sup> to be a prominent vibrational level.

The absorption spectra of the lowest  $4f \rightarrow 5d$  absorption of  $\text{Pr}^{3+}$  in  $\text{BaF}_2$  at liquid-nitrogen temperature are shown in Fig. 5. The spacings between humps are all larger than  $300 \text{ cm}^{-1}$  ( $> \nu_{\text{TO}} > \nu_{\text{TA}}$ ). This indicates that the vibronics observed are not "minor peaks" but "major peaks". The last part of Table II summarizes the peaks in the lowest  $4f \rightarrow 5d$  absorption spectra of  $\text{BaF}_2:\text{Pr}^{3+}$  (from Fig. 5) and shows that values of  $\omega_1 = \Delta\nu_j$  for  $\text{BaF}_2:\text{Pr}^{3+}$  are not as regular as those for  $\text{CaF}_2:\text{Pr}^{3+}$  listed in the other parts of the table.

The spectra of the lowest  $4f \rightarrow 5d$  absorption of  $\text{Pr}^{3+}$  in  $\text{SrF}_2$  have no structure at liquid-nitrogen temperature and are shown in Fig. 6. It is possible that some strains of unknown origin may mask the low-temperature structure.

Previously<sup>4</sup> we have identified the  $^1S_0$  level of  $\text{Pr}^{3+}$

<sup>8</sup> D. L. Wood and W. Kaiser, Phys. Rev. **126**, 2079 (1962). W. Kaiser, W. G. Spitzer, R. H. Kaiser, and L. E. Howarth, *ibid.* **127**, 1950 (1962).

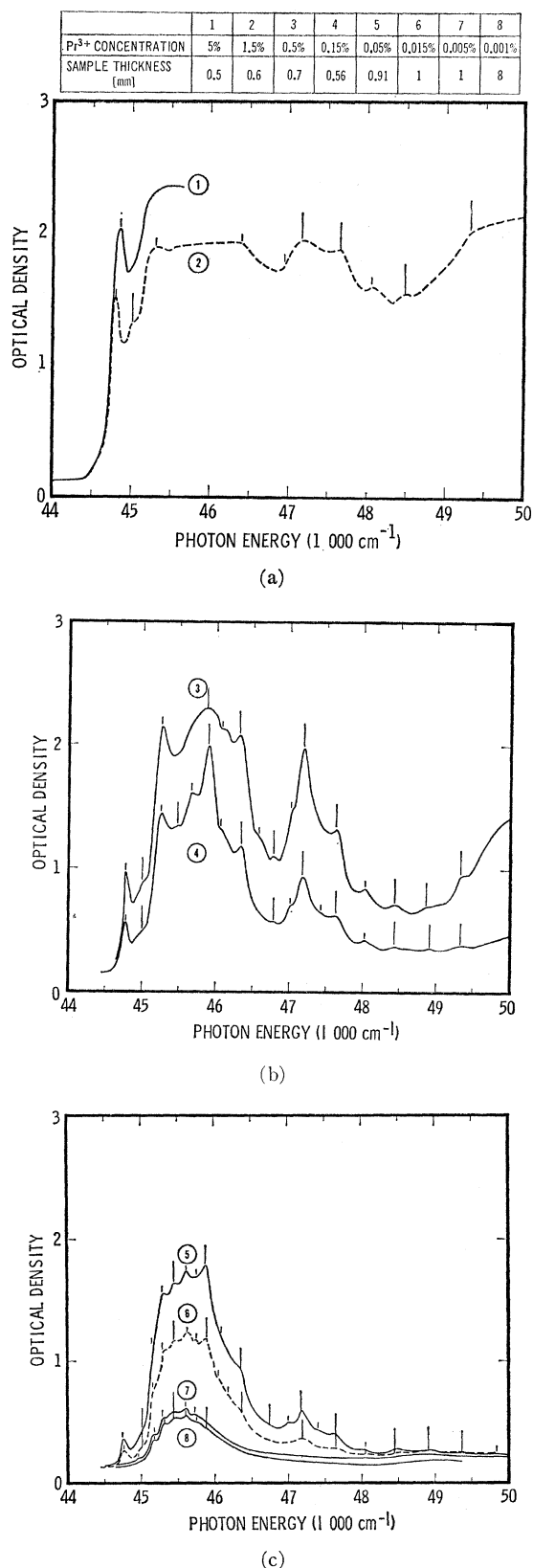


FIG. 4. Lowest  $4f \rightarrow 5d$ -absorption spectra of  $\text{Pr}^{3+}$  in  $\text{CaF}_2$  crystals at liquid-nitrogen temperature.

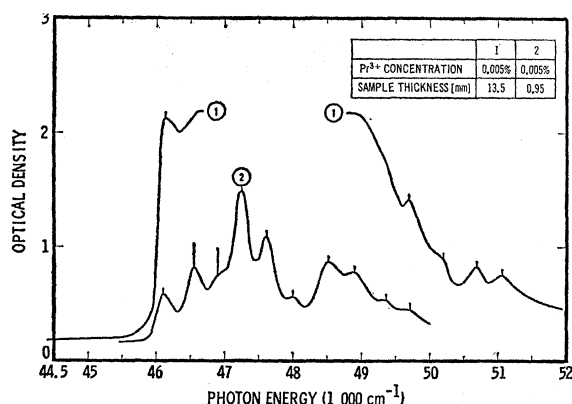


FIG. 5. Lowest  $4f \rightarrow 5d$ -absorption spectra of  $\text{Pr}^{3+}$  in  $\text{BaF}_2$  crystals at liquid-nitrogen temperature.

in  $\text{CaF}_2$  and  $\text{LaF}_3$  crystals. At room temperature, it is a small peak at  $\sim 47\,000\text{ cm}^{-1}$  near the lowest  $4f \rightarrow 5d$  absorption band. The identification<sup>4</sup> of this peak as a transition to the  $^1S_0$  level rather than as part of the  $4f \rightarrow 5d$  transition was based on its shielded character as a  $4f \rightarrow 4f$  transition. In the present work we shall show  $^1S_0$  absorption in  $\text{CaF}_2$  and  $\text{BaF}_2$  more clearly at liquid-nitrogen temperature. In  $\text{CaF}_2$  the  $^1S_0$  level is at  $\sim 47\,200\text{ cm}^{-1}$ , as shown by curves 6 to 2 in Fig. 4 for  $\text{Pr}^{3+}$  concentration 0.015 to 1.5%, respectively, and is followed by a series of vibronics. In  $\text{BaF}_2$  crystal  $^1S_0$  absorption of  $\text{Pr}^{3+}$  appears at  $\sim 47\,240\text{ cm}^{-1}$  and is followed by a series of similar vibronic peaks as shown in Fig. 5 for 0.005%  $\text{Pr}^{3+}$ . The close resemblance between spectra in these two host crystals near and above  $47\,000\text{ cm}^{-1}$  supports the identification of  $^1S_0$  absorption. We have also estimated the values of the oscillator strength of  $^1S_0$  absorption for varying concentration of  $\text{Pr}^{3+}$  in  $\text{CaF}_2$ , from curve 6 for 0.015% to curve 3 for 0.5% in Fig. 4. They are approximately proportional to the product of  $\text{Pr}^{3+}$  concentration times the sample thickness. On the other hand, the main absorption of the lowest  $4f \rightarrow 5d$  band, at photon energy below  $\sim 47\,000\text{ cm}^{-1}$  in Fig. 4, decreases with the increasing concentration of  $\text{Pr}^{3+}$  due to the cluster formation as in the case<sup>1</sup> of  $\text{Ce}^{3+}$  in  $\text{CaF}_2$ . This concentration independence of the absorption cross section of  $^1S_0$  level is again indicative of the shielded character of  $4f \rightarrow 4f$  transition.

### III. CONCENTRATION DEPENDENCE OF $4f \rightarrow 5d$ ABSORPTION OF $\text{Pr}^{3+}$ IN $\text{CaF}_2$ —THE EFFECT OF CRYSTALLINE ENVIRONMENT ON $\text{Pr}^{3+}$ ABSORPTION IN ALKALINE-EARTH FLUORIDES

As in the case of  $\text{Ce}^{3+}$  in Ref. 1, the uv absorption spectra of  $\text{Pr}^{3+}$  in  $\text{CaF}_2$  depends on the concentration of  $\text{Pr}^{3+}$  especially in the region of  $4f \rightarrow 5d$  transitions.<sup>9</sup>

<sup>9</sup> The uv absorption of cluster-ion  $\text{Pr}^{3+}$  in our  $\text{CaF}_2$  samples appears to be more prominent than that of  $\text{Ce}^{3+}$  in Ref. 1 as indicated by comparing the absorption spectra of  $\text{Pr}^{3+}$  and  $\text{Ce}^{3+}$  at comparable concentrations. The smaller ionic size of  $\text{Pr}^{3+}$  may enhance the cluster formation of  $\text{Pr}^{3+}$ -interstitial  $\text{F}^-$  pairs.

Figure 1 shows this concentration effect in a series of uv absorption spectra at varying concentrations from 0.001% to 5%. With increase in  $\text{Pr}^{3+}$  concentration, the  $4f \rightarrow 5d$  bands corresponding to the previously assigned single-ion absorption of  $\text{Pr}^{3+}$  decrease in intensity while the bands in the intermediate-energy region C grow steadily. Following the example<sup>1</sup> of  $\text{Ce}^{3+}$ , we suggest that the absorption in region C is due to  $\text{Pr}^{3+}$  in the cluster formed from several pairs of  $\text{Pr}^{3+}$ -interstitial  $\text{F}^-$  (charge compensator). We assign the hump at  $61\,000\text{ cm}^{-1}$  as the  $t_{2g}$  band and the composite band with peaks at  $54\,000$  and  $56\,000\text{ cm}^{-1}$  as  $e_g$  band, split by supercharge with neighboring  $\text{Pr}^{3+}$ , of cluster-ion  $\text{Pr}^{3+}$ . These absorption bands are shown most clearly by curves 5 and 6 in Fig. 1 for 0.05 and 0.015%  $\text{Pr}^{3+}$ , respectively, at liquid-nitrogen temperature. The crystal-field strength,  $10\text{ Dq}$ , based on this assignment is about  $6000\text{ cm}^{-1}$ , half that of single-ion  $\text{Pr}^{3+}$  in  $\text{CaF}_2$ , and the reduction is due to higher symmetry around the cluster-ion  $\text{Pr}^{3+}$ . The centroid of the  $5d$  levels of the cluster-ion is at  $\sim 59\,200\text{ cm}^{-1}$ . This is about  $2400\text{ cm}^{-1}$  lower than that of single-ion  $\text{Pr}^{3+}$  (see Table I) in  $\text{CaF}_2$  and the difference is presumably due to slightly larger dielectric screening around the cluster ion.

The cluster-ion absorption of  $\text{Pr}^{3+}$  in  $\text{BaF}_2$  is very weak, as mentioned previously. It starts to become evident in a 4-mm-thick  $\text{BaF}_2$  sample containing 0.5%  $\text{Pr}^{3+}$  as shown by two absorption peaks of  $e_g$  at  $54\,000$  and  $56\,700\text{ cm}^{-1}$ , curve 1 in Fig. 3. As in the case<sup>1</sup> of  $\text{Ce}^{3+}$ , we speculate that the large interstitial size available in the  $\text{BaF}_2$  lattice does not encourage cluster formation from  $\text{Pr}^{3+}$ -interstitial  $\text{F}^-$  pairs.

### IV. POSSIBLE $4f \rightarrow 6s$ ABSORPTION OF $\text{Pr}^{3+}$ IN $\text{CaF}_2$

The uv absorption spectra of  $\text{Pr}^{3+}$  in  $\text{CaF}_2$  at photon energies higher than that of  $4f \rightarrow 5d$  are summarized in Fig. 7 for concentrations from 0.001% to 1.5%.

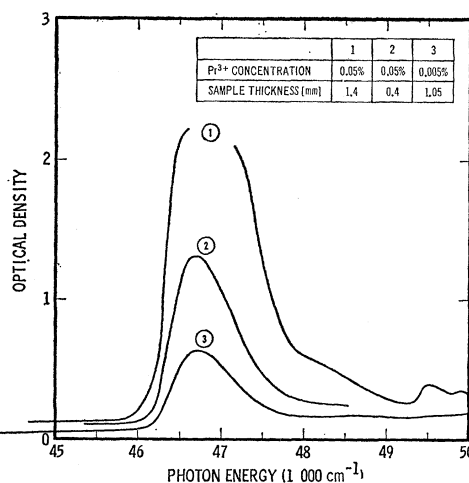
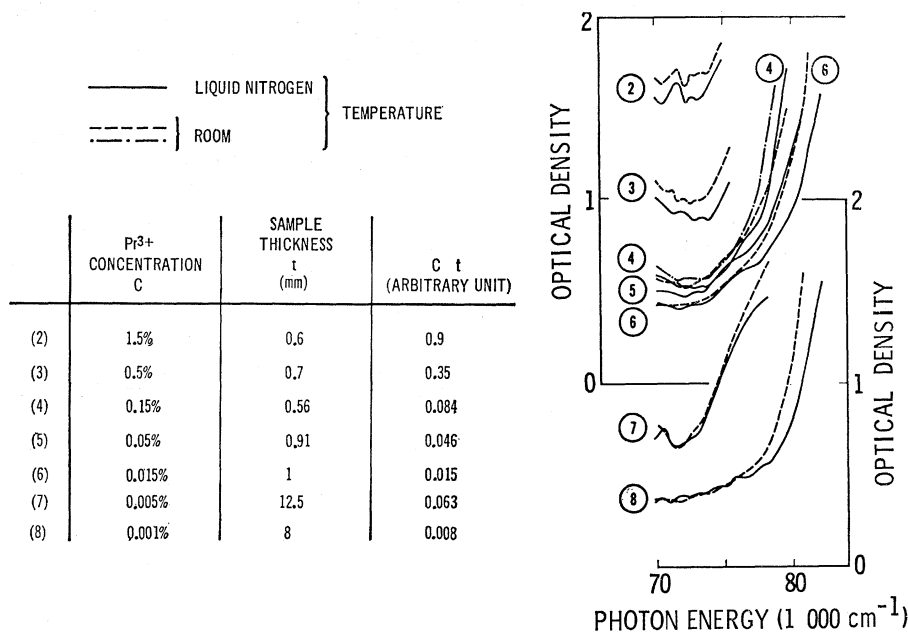


FIG. 6. Lowest  $4f \rightarrow 5d$ -absorption spectra of  $\text{Pr}^{3+}$  in  $\text{SrF}_2$  crystals at liquid-nitrogen temperature.

FIG. 7. Ultraviolet-absorption spectra of  $\text{Pr}^{3+}$  in  $\text{CaF}_2$  crystals near the absorption edge of  $\text{CaF}_2$ .



At liquid-nitrogen temperature a hump at  $\sim 76\,000\text{ cm}^{-1}$  seems to be present in samples of sufficient  $\text{Pr}^{3+}$  concentration (curve 7 for 0.005% to curve 4 for 0.15%  $\text{Pr}^{3+}$  in Fig. 1 or Fig. 7). The absorption at this hump may be assigned to the  $4f \rightarrow 6s$  transition of  $\text{Pr}^{3+}$  in  $\text{CaF}_2$  which is similar to that<sup>1</sup> of  $\text{Ce}^{3+}$  with maximum at  $\sim 70\,000\text{ cm}^{-1}$ .

Table III compares the locations of the interconfigurational transitions  $4f \rightarrow 5d$  and  $4f \rightarrow 6s$  of free-ion<sup>3</sup>  $\text{Pr}^{3+}$  with that of single-ion  $\text{Pr}^{3+}$  in  $\text{CaF}_2$ . The last column in the table shows the ratio of the transition energy of the free ion to that of single-ion  $\text{Pr}^{3+}$  in  $\text{CaF}_2$ . These ratios are comparable to the corresponding values<sup>1</sup> of  $\text{Ce}^{3+}$ .

#### V. RED SHIFT OF ABSORPTION EDGE OF $\text{CaF}_2:\text{Pr}^{3+}$

The absorption edge of  $\text{CaF}_2$  has an apparent red shift as  $\text{Pr}^{3+}$  concentration increases. This is demonstrated, for example, by comparison of the higher apparent edge absorption of curve 5 (0.05%  $\text{Pr}^{3+}$ ) with that of curve 6 (0.015%  $\text{Pr}^{3+}$ ) where samples with comparable thickness but differing by a factor of 3 in concentration ratio were chosen. Following the example<sup>1</sup> of  $\text{Ce}^{3+}$ , we interpret this apparent red shift

of the absorption edge of the host crystal as charge transfer from  $\text{F}^-(2p^6)$  to  $\text{Pr}^{3+}(6s)$ .

#### VI. CONCLUSION

The uv absorption spectra of  $\text{Pr}^{3+}$  in alkaline-earth fluorides are similar to those<sup>1</sup> of  $\text{Ce}^{3+}$  except that  $\text{Pr}^{3+}$  absorption generally occurs at higher energies. This general similarity between the uv absorption spectra of  $\text{Ce}^{3+}$  and  $\text{Pr}^{3+}$  in solids indicates that the crystal field is dominant in the higher configurations  $5d$  and  $6s$  of the rare-earth ions in solids. For  $\text{Pr}^{3+}$  in  $\text{CaF}_2$ , the three interconfigurational transitions are: (1)  $4f \rightarrow 5d$  between  $44\,000$  and  $69\,000\text{ cm}^{-1}$ ; (2) a possible weak  $4f \rightarrow 6s$  absorption at  $\sim 76\,000\text{ cm}^{-1}$ ; and (3) a charge-transfer absorption  $\text{F}^-(2p^6) \rightarrow \text{Pr}^{3+}(6s)$  near  $\sim 80\,000\text{ cm}^{-1}$ . Other effects such as vibronics in the lowest  $4f \rightarrow 5d$  band and their concentration dependence, the effect of cluster formation on the  $4f \rightarrow 5d$  bands, and the crystal effect on the free-ion data are all similar to those of  $\text{Ce}^{3+}$  in alkaline-earth fluorides. The cross section of  $^1S_0$  absorption of  $\text{Pr}^{3+}$  in  $\text{CaF}_2$  is estimated to be concentration-independent, which is consistent with the shielded character of the  $4f \rightarrow 4f$  transition. The  $^1S_0$  absorption and the vibronics are also observed in  $\text{BaF}_2:\text{Pr}^{3+}$ .

#### ACKNOWLEDGMENTS

The author is grateful to Hughes Research Laboratories, where the measurements were performed. He is indebted to the late beloved G. Dorosheski for the tireless computation and construction of numerous graphs. Crystals were supplied by Optovac, Inc. This work is partially supported by the Douglas Independent Research and Development (IRAD) program. J. R. Henderson has kindly read the manuscript.

TABLE III. Energy of centroid of  $4f \rightarrow 5d$  and  $4f \rightarrow 6s$  of free-ion  $\text{Pr}^{3+}$  and single-ion  $\text{Pr}^{3+}$  in  $\text{CaF}_2$ .

Transition	Free-ion $\text{Pr}^{3+}$ ( $\text{cm}^{-1}$ )	Single-ion $\text{Pr}^{3+}$ in $\text{CaF}_2$ ( $\text{cm}^{-1}$ )	(Free-ion $\text{Pr}^{3+}$ ) (Single-ion $\text{Pr}^{3+}$ in $\text{CaF}_2$ )
$4f \rightarrow 5d$	68 100	61 600	1.1
$4f \rightarrow 6s$	102 300	76 000	1.35